Growing degree day measurement of cyst germination rates in the toxic dinoflagellate *Alexandrium catenella*

Alexis D. Fischer* and Michael L. Brosnahan

Biology Department, Woods Hole Oceanographic Institution, Woods Hole, MA 02543, USA

*Corresponding author: afischer@whoi.edu (A.D. Fischer)

266 Woods Hole Rd.

Redfield 332, MS #32

Woods Hole, MA 02543

KEYWORDS: dinoflagellate cyst; germination rate; temperature; *Alexandrium*; degree day; population comparison; oxygen exposure; cumulative distribution function; resting stage

RUNNING TITLE: Dinocyst degree day-based germination rates

Abstract

Blooms of many dinoflagellates, including several harmful algal bloom (HAB) species, are seeded and revived through germination of benthic resting cysts. Temperature is a key determinant of cysts' germination rate, and temperature–germination rate relationships are therefore fundamental to understanding species' germling cell production, cyst bed persistence, and resilience to climate warming. This study measured germination by cysts of the HAB dinoflagellate *Alexandrium catenella* using a growing degree day (*DD*) approach that accounts for time and intensity of warming above a critical temperature. Time courses of germination at different temperatures were fit to lognormal cumulative distribution functions for estimation of the median days to germination. As temperature increased, germination times decreased hyperbolically. *DD* scaling collapsed variability in germination times between temperatures after cysts are oxygenated. A parallel experiment demonstrated stable temperature–rate relationships in cysts collected during different phases of seasonal temperature cycles in situ over three years. Selective pressure for different germination rates is suggested by *DD* scaling of results from prior *A. catenella* germination studies that show consistent differences between populations across a wide range of temperatures. The *DD* model provides an elegant approach to quantify and compare the temperature dependency of germination among populations, between species, and in response to changing environmental conditions.

Importance

Blooms of many dinoflagellates, including several harmful algae species, are initiated by germination of resting cysts, a process whose rate is temperature dependent. This study outlines a growing degree day (*DD*) approach for comparison of rates measured at different temperatures

and through different studies. Germination by cysts of *Alexandrium catenella*, a species that causes paralytic shellfish poisoning, is shown to require a defined amount of warming, measured in *DD*, after cysts are aerated. Scaling by *DD*, the time integral of temperature difference from a critical threshold, enables direct comparison of rates measured at different temperatures and between populations. The approach is used widely in horticulture and is likely to have many other applications for understanding phenology in diverse aquatic microorganisms.

Introduction

During the termination phase of many dinoflagellate blooms, new resting cysts are formed and accumulate in bottom sediments (1). Blooms are revived through cyst germination, a process that produces single diploid planomeiocytes that undergo meiosis to yield new bloom-forming haploid vegetative cells (2). The timing and extent of germination are both critical for bloom initiation by many of these cyst-forming species (3–6).

Several conditions must co-occur for resting cysts to germinate: cysts must be quiescent, a nondormant state in which they will germinate if environmental conditions are favorable (3, 7, 8); oxygen must be present (9, 10); and temperature must be within a suitable range (11, 12). In some species, light is also needed (13). When these prerequisites are met, temperature is the primary determinant of germination rate (14, 15). Temperature–germination rate relationships are therefore fundamental to understanding cyst bed persistence because they control the rate of cyst loss to germination during periods of quiescence. These relationships are also critically important to the timing and success of new bloom initiation.

Cyst to cyst variability in germination rate can be measured within natural populations by synchronizing germination through aeration of quiescent cysts collected from anoxic sediment

(Fig. 1). The distribution of germination times (i.e., the period from a cyst's activation by oxygen exposure to production of a planomeiocyte) reflects the distribution of germination rates within a population. One common measurement method is replicate time course sampling of diluted cyst-rich natural sediments ("slurries"). Anoxic natural sediment samples containing large quantities of quiescent cysts are collected, then aerated through sediment processing and dilution. The resulting slurry is aliquoted to replicate vessels (e.g., flasks, tubes), which are incubated under controlled light and temperature conditions. Individual replicates are removed at defined time intervals and their remaining, ungerminated cysts are counted to reconstruct the germination time course (4, 10, 16) (Fig. 2a). Another method is repeated observation of single cysts. Single cysts are isolated into microwells of a tissue culture plate and each cyst is inspected for germination at regular intervals by microscopy (8, 14, 17) (Fig. 2b). Despite the common use of both slurry- and cyst isolation-based approaches, comparisons of their results from application to a single experimental population had not yet been reported when this study was begun.

Here, germination rates at different temperatures are measured using both the slurry and isolation approaches by cysts of *Alexandrium catenella*, a HAB species that causes paralytic shellfish poisoning (PSP), collected from the Nauset Marsh (Orleans, MA USA). The study applies growing degree days (*DD*) to characterize and compare temperature–germination rates. *DD* are a common heuristic used to predict the phenology and development of terrestrial plants and insects, zooplankton, and even finfish (18–21), and have previously been used to accurately predict the phenology of inshore *A. catenella* blooms (22) and dormancy cycling of *A. catenella* cysts (5, 8). *DD* scaling is further shown to produce strong overlap in median germination rates across several other previously-studied and widely-dispersed cyst populations, demonstrating highly similar temperature–rate relationships for this species. The analytical approach described

here provides a framework to characterize temperature dependence of germination as a trait that can be quantified and compared among globally-dispersed populations, potentially including the resting stages of many other organisms whose germination processes are also synchronized by release from anaerobiosis like *A. catenella* cysts.

Methods

Cyst collections from Nauset Marsh

To isolate the effect of temperature on germination rate, *A. catenella* cysts need to be both quiescent and anaerobically inhibited prior to the start of experiments. These conditions were met by collecting buried cysts and storing them in undisturbed sediment until experiments were begun. The proportion of cysts that were quiescent in each collection was assessed over the course of the rate measurement experiments and through isolation type assays as described by Fischer et al. 2018 (8).

All cysts were collected via sediment coring in Roberts Cove, a shallow area immediately adjacent to the southernmost of three drowned kettle holes within Nauset that host annual *A. catenella* blooms (23). Surficial cyst concentrations in this area are relatively high (typically $>10^3$ cysts cm^{-3} in the 0–3 cm sediment layer) due to heightened export of sexual stage cells during the termination of blooms (1). Bottom water temperature at the collection site was monitored for the duration of the study by a moored, internally-recording HOBO logger (Onset Computer Corporation; Fig. 3a). Sediment cores were capped after collection and brought to our laboratory in Woods Hole, MA in an upright orientation, shielded from light, and maintained near their in situ temperature.

115 After sediment cores were brought to the laboratory, headwater was aspirated and the
116 cores were extruded. Cysts were collected from the sediment-water interface down to 3 cm.
117 Because cyst concentrations within the 0–3 cm layer are generally greater subsurface (24, 25)
118 and only a fraction of cysts from the top surface mm germinate from undisturbed sediment (25),
119 the overwhelming majority of cysts collected for these experiments were presumed to be
120 inhibited by anaerobiosis (10). The collected cysts were from several different year classes due
121 to physical mixing and bioturbation processes in this environment.
122
123 **Germination rate measurements across different temperatures**
124 Rate measurements across temperatures were first evaluated through a large slurry
125 experiment. In this design, the time course of germination is reconstructed from the loss of cysts
126 observed in replicate cyst samples removed and counted at different timepoints (Fig. 2a). All
127 cysts for the experiment were taken from a total of seven sediment cores, collected on 05 March
128 2014. These cores provided approximately 150 cm^{-3} of anoxic sediment, which was brought to a
129 total volume of 1.2 L through addition of f/2 medium. The resulting slurry was homogenized and
130 aliquoted in 10 mL volumes to 250-mL glass flasks (106 total), then diluted further through
131 addition of 50 mL of f/2 medium and swirled to mix and aerate as described by Anderson et al.
132 2005 (16). All manipulations were carried out inside a 4°C walk-in refrigerator to maintain the
133 temperature observed in Nauset at the time of collection.
134 After aliquoting, a total of six flasks were immediately processed for counting to estimate
135 the mean initial number of cysts in each of the aliquots. The remaining one hundred flasks were
136 arrayed in sets of 20 in five different incubators set to 2, 4, 8, 10, and 12°C on a 14:10 light:dark
137 cycle (150 μE m^{-2} s^{-1} photon flux density). These temperatures approximate the range of Nauset

138 bottom water temperatures in the winter and spring when cysts are quiescent, and therefore
139 germinable (8) (Fig. 3). Sampling intervals varied between incubation temperatures to ensure
140 adequate coverage of the germination time course, e.g., from 3 to 12 days at the coldest
141 temperatures from 2 to 4 days at the warmest. At each sampling timepoint, flasks were removed
142 from the experiment for counting. For most timepoints (~80%), flasks were removed and
143 counted in duplicate, but occasionally only single flasks were taken to conserve samples.
144 Remaining, uncounted slurry-filled flasks were thoroughly mixed once per week to provide
145 comparable light exposure to all cysts.
146 The contents of slurry flasks were prepared for counting by primulin staining as
147 described by Yamaguchi et al. 1995 (26). Cyst samples were fixed with formalin (5% v/v) at 4ºC
148 for at least 30 min, and centrifuged (3000 x *g*, 5 min) before formalin was exchanged with cold
149 methanol and stored at 20ºC for at least 48 h for pigment extraction. Next, samples were
150 centrifuged (3000 x *g*, 5 min), then methanol exchanged with 10 mL distilled-deionized water.
151 Samples were centrifuged again and pellets resuspended in 2 mL staining solution (2.0 mg
152 primulin mL^{-1} in distilled-deionized water). After staining for 1 hr at 4ºC on a laboratory shaker
153 (Barnstead Thermolyne Labquake), samples were centrifuged, decanted, and the total volume
154 was brought to either 5 or 10 mL with distilled-deionized water – the 5 mL resuspension volume
155 was used for flasks processed at the end of the experiment that had fewer cysts. For each flask
156 sample, all of the cysts in a 1 mL subsample were counted under a Zeiss Imager microscope
157 using blue light epifluorescence at 100x magnification with Zeiss filter set 09 (excitation 450–
158 490 nm, dichroic 510 nm, emission 515 nm long pass). *A. catenella* cysts were identified by the
159 "lime-green" fluorescence of their primulin-stain and their characteristic pill or capsule shape
160 (55–60 μm long and 20–25 μm in diameter; Fig. 4). The fraction of cysts that germinated during

each time interval was estimated as the difference between the mean initial cysts per flask and the mean cysts per flask remaining cysts at each sampling time.

Effect of temperature conditioning on the germination rate

The question of whether differences in the recent environmental history (e.g., temperature) might affect the observed distribution of cysts' germination rates was addressed through isolation type experiments conducted over three years during months when Nauset cyst beds were nearly fully quiescent. In these experiments, smaller samples of cysts were isolated from sediment samples and their germination monitored through weekly inspections at temperatures that were similar to those observed in situ during the same period.

Sediment for isolation experiments was collected in 2013, 2014, and 2015 during the first weeks of February, March, April, and May when cysts were known to be quiescent (Fig. 3b). A 5 cm^3 subsample of anoxic surface sediment was disaggregated by sonication (Branson Sonifier 250; 1 min at 40%), and then passed through a series of Nitex sieves to isolate the cyst-containing 20–80 μm size fraction (27). The resulting sample was resuspended in 0.2 μm filtered seawater for further enrichment via density gradient centrifugation using a method described by Schwinghamer et al. 1991 (28). *A. catenella* cyst densities range from approximately 1.15 to 1.30 g cm^{-3} so a heavy cushion solution was prepared from colloidal silica (Nalco 1060, Nalco Chemical Co., Chicago, IL) and combined with sucrose to achieve a final density of 1.40 g cm^{-3}. Cyst suspensions were underlaid with the colloidal silica suspension then centrifuged 1600 x *g* for 15 min at room temperature. Cysts were collected from the cushion/sediment suspension interface by pipette, then washed over a 20 μm Nitex sieve with 0.2 μm filtered seawater. Sieve contents were backwashed into a 15 mL centrifuge tube and 1 mL aliquots were pipetted into a

184 Sedgewick-Rafter counting chamber from which cysts could be easily identified under a Zeiss
185 Axioskop upright microscope at 100x magnification.
186 For each monthly germination assay, clutches of approximately 30 cysts with a healthy
187 appearance (starch granules present, visible red eyespot, golden to brown coloration; Fig. 4a–c)
188 were transferred by micropipette to individual wells of 96-well tissue culture plates and
189 incubated at two temperatures: the approximate in situ bottom water temperature at the time of
190 collection (2–12ºC) and 15ºC, an optimum control temperature at which most cysts will
191 germinate within one week if viable and quiescent (Fig. 3) (8). In 2013–2014, the incubators
192 used in April and May were discovered to be warmer than their nominal set points – ~9ºC
193 instead of 7ºC, and ~12ºC instead of 11ºC – but this was resolved by 2015. Our analysis was
194 adjusted to reflect the true temperature experienced by cysts during the respective incubations.
195 Microwell plates were preloaded with 200 μL of modified f/2-Si medium and plates were
196 sealed after cyst isolation to limit evaporative loss of media (29). In all incubations, cysts
197 experienced a 14:10 light:dark cycle (150 μE m^{-2} s^{-1} photon flux density). Individual cysts were
198 inspected for germination on a weekly basis under 100x magnification and scored as having
199 germinated based on the presence of vegetative *A. catenella* cells or an empty cyst cell wall. As
200 with the slurry experiment, the isolation experiment was terminated once no new germination
201 had been observed for 2 consecutive weeks and a minimum of 4 weeks had elapsed. A small
202 number of ungerminated cysts remained in the microwell plate at the termination of all isolation
203 experiments. In comparison to the healthy appearances of cysts at the start of experiments, these
204 remaining ungerminated cysts had unhealthy appearances (Fig. 4), and were therefore
205 determined to have died. “Unhealthy” visual cues included blebbing, blackened coloration, and
206 eyespots that were difficult to distinguish. Germinated cysts were divided by the total isolated

cysts to calculate the maximum cumulative germination, G_{max}, for each experiment. Results were compared to cumulative germination observed in the subset of slurry incubations in which no new germination was observed over at least the last two weeks of their incubation (temperatures >2ºC).

Fitting germination time course curves

In analyzing germination time course data, it is important to consider sources of measurement uncertainty. For the slurry approach, data take the form of counts and observational units (cyst samples/timepoints) are independent (Fig. 2a). In the isolation approach, the same cyst is repeatedly inspected at successive times, producing "time-to-event" type data that are commonly considered in survival analyses (Fig. 2b). In both approaches, the exact germination time of an individual cyst is not observed or recorded but instead occurs at some time prior to a final observation timepoint. Isolation experiments better constrain individual cyst germination times but exact intervals are only known to be sometime between an experiment's final and penultimate observations (i.e., interval-censored data).

Cumulative germination by slurry and isolation samples is sigmoidal with time and were fit to several, common cumulative distribution functions (CDFs). Maximum likelihood estimation was used to fit Nauset time course data to several probability distribution models including gamma, loglogistic, lognormal, and Weibull distributions. Of these, lognormal distributions best described cumulative germination data and were used to interpolate median germination times where required for subsequent analyses.

For the slurry dataset, cumulative germination proportions at each timepoint were determined by dividing the remaining number of cysts by their initial number. For each

experiment, cumulative germination was fit to a lognormal distribution using maximum likelihood estimation of the median with the nonlinear solver function *fminsearch* in MATLAB (MathWorks, Natick, MA).

Because cyst isolation data are interval censored, a slightly different maximum likelihood model was applied that accounted for both minimum and maximum estimates of each cysts' time to germination (30). Ideally, the status of each cyst at each timepoint would have been tracked with regard to four possible outcomes: viable-germinated, viable-ungerminated-quiescent, viable-ungerminated-dormant, or dead-ungerminated. However, cyst death was only recorded at the end of experiments, in part because the timing of cyst death is unclear. Visual cues of unhealthiness may develop some unknown time before or after a cyst expires (Fig. 4d). In other cases, no visual cue may be present that allows differentiation of viable, dormant cysts from those that have died. Some fraction of cysts collected from environmental samples inevitably expire due to their handling. We noted substantially higher cumulative germination in slurry experiments than in isolation experiments undertaken with material from the same set of sediment cores (05 March 2014) and consistently lower cumulative germination in isolation experiments overall. Based on these observations, we concluded that processing steps unique to the isolation experiment (e.g., sonication) likely injured a portion of the cysts. For this reason, cysts that had not germinated at the end of isolation trials were assumed to be dead and were discounted in estimates of cumulative germination. Censored data were then fit to a lognormal CDF distribution based on maximum likelihood with the *lognfitc* function in MATLAB (31).

Degree day-scaling of the temperature–germination rate relationship

As expected, warmer incubation temperatures drove faster germination. This was quantified by the median germination time or t_{50}, which was estimated from lognormal fits of the respective temperature incubations. Because the relationship between temperature and t_{50} was hyperbolic, scaling by *DD* was explored as a means to compare experiments performed at different incubation temperatures.

For each experimental timepoint, *DD* were calculated as the integral over time (t) of temperature above a threshold (T_{crit}):

$$DD(t) = \sum_{i=t_0}^{t} (T_i - T_{crit})\Delta t \qquad \text{Eq. 1}$$

where t_0 is the starting time of the experiment, T_i is the daily temperature, and T_{crit} is the lower critical temperature below which germination does not occur. For each independent temperature experiment, the median degree days to germination (DD_{50}) was considered the most representative measure of a cyst cohort's central tendency and was calculated as:

$$DD_{50} = (T_i - T_{crit})t_{50} \qquad \text{Eq. 2}$$

Because the lower physiological limit below which germination does not occur was unknown for the Nauset *A. catenella* cyst population, we explored T_{crit} values between -1 and 1ºC. Values near 0ºC minimized variance in DD_{50} across all temperatures tested in both slurry and isolation experiments. This temperature was therefore used for T_{crit} in all *DD* estimates from experiments conducted through this study.

Preliminary application of *DD* scaling to other populations

As an initial assessment of whether *DD* scaling could be used to quantify temperature–germination rate relationship in other *A. catenella* populations, the same mathematical approach was applied to the previously-published slurry experiments of Anderson et al. 2005 and Moore et al. 2015. The former study assessed germination rates at temperatures between 2 and 15ºC by cyst from the open coastal regions of the western and eastern Gulf of Maine (GOM) (16), and the latter at temperatures between 10 and 20ºC by cysts from Bellingham Bay (Puget Sound, WA) (4). *DD* were calculated using T_{crit} of 0ºC and results were fit to lognormal CDF distributions just as for Nauset to estimate t_{50} and DD_{50} values for the GOM and Puget Sound populations.

Results

Slurry-based assessment of temperature-germination rate relationship

Across all slurry experiments, germination rates increased with temperature through the full range tested (2, 4, 8, 10, 12ºC). This was most evident through comparisons of cumulative germination at early timepoints (Fig. 5a). For example, within the initial 8 days, cysts incubated at 8ºC attained 15% cumulative germination, whereas cysts incubated at 12ºC attained 87% cumulative germination. There was also an initial lag, or time delay, before cysts began to germinate that scaled with temperature; i.e., there was a shorter lag at warmer temperatures and a longer lag at colder temperatures. For all temperature experiments, cysts had a mean G_{max} of 99% (SD = 0.6), demonstrating that essentially all cysts collected in March 2014 were viable and quiescent.

Fits of cumulative germination curves to lognormal CDFs accurately predicted cumulative germination of all but the fastest cysts that germinated during the initial lag phase,

296 which tended to be underestimated (Fig. 5). Curves were better defined in the lower temperature
297 experiments than at higher ones due to a larger number of observations at intermediate levels of
298 cumulative germination. For example, in the 2ºC experiment, 9 timepoints recorded less than
299 90% cumulative germination, but in the 12ºC experiment, only 2 timepoints were less than the
300 90% threshold. Median germination times (t_{50}) estimated from all fits were hyperbolically related
301 to incubation temperature with values ranging from 6 days at 12ºC to 44 days at 2ºC (Fig. 6).
302 Differences in procession toward complete germination collapse after *DD* scaling (Fig.
303 5b) with remarkably low variance among DD_{50} estimates across individual temperature
304 experiments (mean ± SD, 77 ± 8 DD). Similarly, lognormal fitting of all *DD*-scaled data
305 produced a DD_{50} estimate of 78 DD. Analyses of residuals of the *DD*-scaled data to the
306 respective lognormal distributions (individual and combined) also showed strong agreement with
307 the lognormal CDF model, except at the lowest levels of cumulative germination where models
308 tended to underestimate observed cumulative germination levels.
309
310 **Assessment of temperature–germination rate dependence on in situ conditioning**
311 Isolation experiments measured germination rates of cysts collected from Nauset over
312 three years during months when they were typically quiescent (February–May, 2013–2015) to
313 assess whether recent environmental history might affect observed distributions of germination
314 rates. Much like slurry experiments, time to germination was inversely proportional to
315 temperature but the maximum levels of cumulative germination were notably lower overall
316 (mean G_{max} ± SD, 76 ± 9%). As further comparison, the isolation experiment conducted with the
317 same March 2014 sediment as the slurry experiments only reached a G_{max} of 62%. Cysts that did
318 not germinate during isolation experiments frequently turned black, displayed blebbing, and/or

319 produced green autofluorescence at the end of experiments, all of which are morphological
320 indicators of cyst death (Fig. 4d). Effects of the year and month of a cyst cohort on their G_{max}
321 were tested through application of a Pearson chi-squared test to data from 15ºC control
322 incubations. Neither differences between years (X^2 = 24, n = 12, p = .35) nor months (X^2 = 36, n
323 = 12, p = .33) were significant and therefore all monthly cyst collections were considered to have
324 equivalent viabilities.
325 No effects from different months or years of cyst collection were apparent after *DD*
326 scaling of isolation experiment results. Estimates of cumulative germination generally
327 overlapped those from the slurry-based temperature experiments (Fig. 7) and the DD_{50} from
328 fitting to a single lognormal CDF distribution was 77 DD (*SD* = 19), essentially identical to
329 estimates derived from slurry experiment data (Fig. 5). Given this consistency between slurry
330 and isolation time courses, it was concluded that distributions in germination rates were
331 insensitive to seasonally changing environmental conditions experienced in Nauset.
332 Likewise, slurry-derived germination times from Puget Sound and the eastern and
333 western GOM were highly similar to those from Nauset after *DD* scaling. In each case,
334 germination time courses were well approximated using lognormal CDF functions, and derived
335 t_{50} values were hyperbolically related to incubation temperatures (Fig. 6). From application of a
336 common T_{crit} of 0ºC, Puget Sound cysts appeared to require the fewest *DD* to germinate,
337 followed by Nauset, western GOM, and eastern GOM cysts.
338
339 ***Discussion***
340 This study successfully demonstrated a *DD*-based analytical approach for comparison of
341 germination rates by *A. catenella* cysts measured at different temperatures and using different

experimental approaches. Differences between respective temperature incubations were eliminated after *DD* scaling, revealing a highly-consistent distribution of germination times among natural *A. catenella* cysts from Nauset throughout quiescent periods and over multiple years (Figs. 5 & 7). Likewise, *DD* scaling collapsed variability in cyst germination times from previously published studies of populations from Puget Sound and the Gulf of Maine (Fig. 6). Consistent differences between the Nauset Marsh, Puget Sound, and GOM populations show how *DD* frameworks may facilitate comparison of different populations, studies, and perhaps even different species. The results further show how *DD* relationships can improve characterization of germination processes for better understanding the timing and magnitude of germination fluxes across different cyst habitats and in response to changing ocean bottom conditions.

Stability of germination rates in a natural population

The strong similarity of germination rates measured from quiescent *A. catenella* cysts sampled from Nauset in different months and years indicates that the rate distribution is a fixed characteristic of the population that does not respond to conditioning in situ (Figs. 5 & 7). Cysts measured through isolation experiments were different mixtures of year classes, experiencing different conditions at the time of their formation, and different temperature histories leading up to their collection for isolation experiments. Yet, the distribution of germination rates, once scaled by *DD*, appears to have barely been impacted (if at all).

Also noteworthy is the strong similarity of estimates from the slurry- and isolation-based methods (Fig. 7). To our knowledge, this is the first study that has directly compared slurry- and isolation-based approaches for measuring germination rates in a microbial eukaryote. The slurry

365 design has several practical advantages relative to the isolation approach. These include the
366 ability to more easily record germination at high frequency and to maintain consistent incubation
367 temperatures through the duration of an experiment. In contrast, isolation-based measurements
368 require repeated inspections of individual cysts which involves removal from incubators for
369 observation in many laboratories. These inspections can drive deviations from nominal
370 incubation temperatures, a significant concern especially for the coldest incubations which can
371 extend for several months.

372 This type of temperature stress may have contributed to observed differences in
373 maximum cumulative germination observed between slurry and isolation experiments. Other
374 notable differences between these approaches include sonication, density gradient enrichment,
375 and micropipette manipulation of individual cysts. Prior applications of isolation type methods to
376 cysts from coastal GOM beds have yielded cumulative maximum germination levels exceeding
377 90% (7, 32), but these samples generally consist of much finer sediment than is present in Nauset
378 (33). Higher fractions of coarse sand grains in Nauset cores may have injured cysts during the
379 initial sonication step of the isolation procedure, leading to reductions in their viability relative to
380 slurry experiments (mean G_{max} ± SD, slurry = 99 ± 0.6%, isolation = 76 ± 9%). The significantly
381 greater mortality in isolation experiments precluded a rigorous statistical comparison of the two
382 methods, but they still produced nearly equivalent estimates of median germination time (77 and
383 78 DD for isolation and slurry approaches, respectively; Fig. 7). Future experiments applying
384 repeated measures designs (like the isolation approach) should take care to document the timing
385 and extent of cyst death through the full course of incubations or take steps to eliminate viability
386 differences between methods because these have the potential to bias estimates of cumulative
387 processes like germination (30). Limited divergence between the two methods was apparent only

among the fastest germinating fraction of cysts. Specifically, a higher proportion germinated in the earliest stages of slurry experiments than was observed in the isolation experiments (Figs. 5 & 7).

Prior studies have observed sigmoid-type (S-shaped) time course patterns of cumulative germination in other *A. catenella* cyst populations (4, 10, 14, 16) and in many terrestrial plant seeds (34). Past *A. catenella* studies pointed out the initial lag in germination (visible in the first part of the time course curve) and attributed its presence to a cyst acclimation period associated with rapid changes in temperature or storage conditions (4, 16). It is clear from the present study that the initial lag simply reflects the combined effects of germination being initiated through oxygenation and the variance of rates within a population. The initial lag shape is produced because only the fastest cysts germinate at the start of an experiment, as they require the fewest *DD* to germinate. *DD* scaling also enables consideration of the complete set of recorded germination times to extract estimates of mean or median germination rates. This is in contrast to past studies that extracted linear segments of cumulative germination time courses (4, 16) or fit first-order exponential functions (10, 14) to estimate rates at different temperatures.

The current study fits lognormal CDFs to time course data to estimate median germination times, but the *DD* framework also enables explicit description of the distribution of germination rates found in natural populations of cysts. Accounting for the full range of germination responses, from the fastest to the slowest cysts, can inform future studies that aim to quantify the in situ germling flux and the potential resilience of cyst populations faced with rapidly-changing ocean bottom water conditions. Future work will be aimed at more rigorously fitting slurry data for pairwise statistical comparisons and for more accurate estimation of the full distribution of germination rates in different populations. The latter enables direct estimation of

411 mean germination times expressed in *DD*, which is a more typical summary statistic for
412 investigations of cyst bed behavior across a range of bottom water temperatures.
413
414 **Initial population comparisons**
415 Blooms of *A. catenella* occur in a variety of habitats ranging from temperate to the
416 Arctic, and from estuarine embayments to open coastal waters, so temperature–germination rate
417 relationship comparisons across populations can have broad implications for species ecology and
418 biogeography. These comparisons may also provide insights into how different populations will
419 respond to a changing climate. Germination rate differences within and between populations can
420 underlie a population's ability to adapt and/or acclimate. However, at the time of this study, an
421 approach to quantitatively compare cyst germination rates of different dinoflagellate populations
422 did not exist, thus the framework provided by this study represents an important step forward.
423 The stability of germination rate distributions observed across experiments with Nauset
424 *A. catenella* cysts suggests that the distribution of this trait is shaped by environmental selection
425 on populations. In habitats that have periods of favorable conditions typically associated with
426 highly seasonal temperature shifts, such as a warmer spring following a cold winter, selection
427 may favor slower germination as this could ensure that germlings emerge when conditions are
428 more consistently favorable for bloom development. Thus, cysts would respond more slowly to
429 short, unseasonable fluctuations in temperature, such as an anomalous warm spell during winter.
430 Alternatively, in habitats with less seasonality that have shorter or irregular windows of
431 favorable conditions for bloom development, selection may favor rapid germination, as this
432 would enable cysts to respond quickly to ephemeral conditions.

433 *DD* scaling of germination time course data from other populations also demonstrates
434 how this analytical approach may be used to compare results from different laboratories and
435 choices of incubation temperature. The selected germination studies by Anderson et al. 2005 and
436 Moore et al. 2015 were conducted over a decade apart, targeted different *A. catenella*
437 populations, and investigated different incubation temperatures (4, 16). Cumulative germination
438 by all of these populations and at all temperatures was well described by lognormal CDFs.
439 Estimates of t_{50} were also hyperbolically related to incubation temperature (Fig. 6), such that
440 Puget Sound cysts appear to require the fewest *DD* to germinate, followed by Nauset and then
441 GOM cysts. Faster germination of Puget Sound cysts may reflect the relatively modest
442 temperature seasonality of this system compared to Nauset and GOM. Habitats with weaker
443 seasonality do not synchronize dormancy cycles to the same extent (5) and are associated with a
444 long season of PSP risk (i.e., potential for blooms) (35).
445 It remains to be shown if germination differences are statistically significant, and if so,
446 how differences in germination rates reflect differences in physical, chemical, or biological
447 conditions across these and other globally-distributed *A. catenella* habitats. Nauset and Puget
448 Sound are both relatively shallow, inshore habitats where benthic cyst beds experience direct
449 environmental signals associated with the onset of conditions supporting bloom development. In
450 contrast, GOM cyst beds are located in open coastal waters at depths that isolate them from
451 conditions in overlying euphotic waters (14). Germling fluxes from each of these cyst beds are
452 critical for initiation of new blooms, and bloom timing and duration vary in ways that suggest
453 linkage to cyst bed activity (5, 6).
454 In many regions, warming ocean waters are increasingly impacting bottom water
455 temperatures that can drive dramatic changes in germling production from cyst beds (36).

Therefore, several important questions that remain to be addressed include: (1) How may faster germination convey advantages in one habitat but not another? (2) Which mechanisms drive selection for germination rates in different habitats and over what time scale can populations shift in the face of rapidly-changing coastal conditions? and (3) How and to what extent do populations retain diversity and variance among cysts with respect to their germination rates? To effectively connect populations' germination physiology to biogeography, future work is needed to quantify population variance, to determine an approach to derive a population's T_{crit} value for *DD* calculations, and to develop statistical approaches to compare derived parameters.

Synchronization reveals degree day relationships

Synchronization through aeration of cysts was key to revealing the distribution of times required for individual cysts to germinate. Typical precautions were taken throughout sample collections for this study to prevent oxygen exposure prior to all cyst incubations. These included transport of cysts from the field in sediment cores and removal of any material that may have been exposed to air before creation of sediment slurries or isolation of cysts to microwell plates. Because cysts only start the germination process after exposure to air, these precautions ensured that initiation of germination was synchronized.

Inhibition of germination by anaerobiosis is by no means unique to *A. catenella* cysts. Diverse microbes and even aquatic animals produce similar resting stages and in many cases their germination or hatching requires oxygen. These include many species of dinoflagellates (9, 10), diatoms (37), cyanobacteria (38), and zooplankton (39, 40). For those species that are activated through oxygen exposure, a similar experimental approach may synchronize natural samples and enable recording of germination or hatching response time distributions.

Many but not all species also experience dormancy, a physiological state that inhibits germination even when conditions are otherwise favorable. Synchronization of *A. catenella* cyst dormancy cycles revealed that the passage from quiescence into dormancy is well described by *DD* (5). Similarly, passage from dormancy into quiescence follows a comparable, chilling-unit relationship (8). When cysts experience annual cycles of seasonal temperatures, intervals of dormancy and quiescence are increasingly phased such that inshore regions that experience the largest differences between peak summertime and minimum wintertime temperatures, like Nauset, are essentially synchronized (5). Seasonally-induced synchronization of the Nauset cyst population also enables *DD*-based prediction of bloom phenology in the Nauset system (22). Future experiments investigating the applicability of *DD* to physiological processes and phenology of other species should consider population synchronicity in their design and analysis. *DD*-type relationships will be obscured in processes that are not gated or otherwise synchronized in some way. Likewise, dormancy (in species where it occurs) may obscure or prevent measurements of germination time or other processes.

Application for estimating in situ germling flux

Germination is one of several temperature- and season-influenced processes that drive germling cell production from cyst beds. Other important processes include microbial respiration, sediment mixing, resuspension, and bioturbation, all of which control the exposure of buried cysts to oxygen and therefore the initiation of germination. Microbial respiration can be described by *DD* relationships in some systems (41), and increases in response to seasonal detrital inputs (42). Mixing processes, such as bioturbation and resuspension (by waves and currents), influences the vertical distribution of cysts within sediment and the tortuosity of paths

502 that germling cells must navigate to reach the water column (6, 33). Accurate estimation of
503 fluxes must consider each of these processes and is therefore complex (43). Dinoflagellate
504 germling fluxes are also challenging to measure in situ, so only a small number of observations
505 have been reported to date (44, 45). This lack of data limits efforts to constrain the interacting
506 effects of temperature on mixing, resuspension, and oxygen consumption within sediments on
507 germination and germling flux.

508 It is still possible to hypothesize cyst beds' response to changing bottom water conditions
509 under the assumption that fluxes are driven primarily by germination. Through application of *DD*
510 scaling, changes in the timing, intensity, and duration of cyst germination were recently
511 estimated for a massive *A. catenella* cyst bed across the Chukchi Sea (36). The authors applied a
512 generalized temperature–germination rate relationship from observations of several North
513 American cyst populations. Due to observed changes in bottom water temperatures over the last
514 two decades, total germling production may have increased nearly two-fold and advanced up to
515 three weeks earlier in the year. The latter phenological shift would represent a substantial
516 expansion of the window for blooms to develop in this high latitude region. Still, other
517 interacting effects of temperature could mitigate or magnify the direct effects of warming on
518 germination rates. The potential scale of Chukchi blooms and danger posed by PSP to human
519 and animal populations calls for further investigations that link temperature change to cyst bed
520 activity.

521 Uncertainty regarding how changing water temperatures may affect bioturbation,
522 microbial respiration, and other benthic processes underscores the need for more studies that
523 quantify their relationships with temperature. Each of these processes has direct impacts on the
524 activity of many benthic resting stages that seed and shape the diversity and structure of plankton

communities in overlying waters. The *DD* framework used in this study has already been shown to be useful in characterizing a wide range of biological phenomena. Many new applications are yet to be described in marine systems.

References

1. Brosnahan ML, Ralston DK, Fischer AD, Solow AR, Anderson DM. 2017. Bloom termination of the toxic dinoflagellate *Alexandrium catenella*: Vertical migration behavior, sediment infiltration, and benthic cyst yield. Limnol Oceanogr 62:2829–2849.
2. Von Stosch HA. 1973. Observations on vegetative reproduction and sexual life cycles of two freshwater dinoflagellates, *Gymnodinium pseudopalustre* Schiller and *Woloszynskia apiculata* sp. nov. Br Phycol J 8:105–134.
3. Lopez CB, Karim A, Murasko S, Marot M, Smith CG, Corcoran AA. 2019. Temperature mediates secondary dormancy in resting cysts of *Pyrodinium bahamense* (Dinophyceae). J Phycol 55:924–935.
4. Moore SK, Bill BD, Hay LR, Emenegger J, Eldred KC, Greengrove CL, Masura JE, Anderson DM. 2015. Factors regulating excystment of *Alexandrium* in Puget Sound, WA, USA. Harmful Algae 43:103–110.
5. Brosnahan ML, Fischer AD, Lopez CB, Moore SK, Anderson DM. 2020. Cyst-forming dinoflagellates in a warming climate. Harmful Algae 91.
6. Anderson DM, Keafer BA, Kleindinst JL, McGillicuddy DJ, Martin JL, Norton K, Pilskaln CH, Smith JL, Sherwood CR, Butman B. 2014. *Alexandrium fundyense* cysts in the Gulf of Maine: Long-term time series of abundance and distribution, and linkages to past and future blooms. Deep Res Part II Top Stud Oceanogr 103:6–26.

548 7. Anderson DM, Keafer BA. 1987. An endogenous annual clock in the toxic marine
549 dinoflagellate *Gonyaulax tamarensis*. Nature 325:616–617.
550 8. Fischer AD, Brosnahan ML, Anderson DM. 2018. Quantitative Response of Alexandrium
551 catenella Cyst Dormancy to Cold Exposure. Protist 169:645–661.
552 9. Kremp A, Anderson DM. 2000. Factors regulating germination of resting cysts of the
553 spring bloom dinoflagellate *Scrippsiella hangoei* from the northern Baltic Sea. J Plankton
554 Res 22:1311–1327.
555 10. Anderson DM, Taylor CD, Armbrust EV. 1987. The effects of darkness and anaerobiosis
556 on dinoflagellate cyst germination. Limnol Oceanogr 32:340–351.
557 11. Anderson DM, Morel FMM. 1979. The seeding of two red tide blooms by the germination
558 of benthic *Gonyaulax tamarensis* hypnocysts. Estuar Coast Mar Sci 8:279–293.
559 12. Anderson DM, Rengefors K. 2006. Community assembly and seasonal succession of
560 marine dinoflagellates in a temperate estuary: The importance of life cycle events. Limnol
561 Oceanogr 51:860–873.
562 13. Binder BJ, Anderson DM. 1986. Green light-mediated photomorphogenesis in a
563 dinoflagellate resting cyst. Nature 322:659–661.
564 14. Vahtera E, Crespo BG, McGillicuddy DJ, Olli K, Anderson DM. 2014. *Alexandrium*
565 *fundyense* cyst viability and germling survival in light vs. dark at a constant low
566 temperature. Deep Res Part II Top Stud Oceanogr 103:112–119.
567 15. Pfiester LA, Anderson DM. 1987. Dinoflagellate Reproduction, p. 611–648. *In* Taylor, FJ.
568 (ed.), The Biology of Dinoflagellates. Blackwell Scientific Publications.
569 16. Anderson DM, Stock CA, Keafer BA, Bronzino Nelson A, McGillicuddy DJ, Keller M,
570 Thompson B, Matrai PA, Martin J. 2005. *Alexandrium fundyense* cyst dynamics in the

571 Gulf of Maine. Deep Res Part II Top Stud Oceanogr 52:2522–2542.
572 17. Anderson DM. 1980. Effects of temperature conditioning on development and
573 germination of *Gonyaulax tamarensis* (Dinophyceae) hypnozygotes. J Phycol 16:166–
574 172.
575 18. Trudgill DL, Squire GR, Thompson K. 2000. A thermal time basis for comparing the
576 germination requirements of some British herbaceous plants. New Phytol 145:107–114.
577 19. Mackas DL, Goldblatt R, Lewis AG. 1998. Interdecadal variation in developmental timing
578 of *Neocalanus plumchrus* populations at Ocean Station P in the subarctic North Pacific.
579 Can J Fish Aquat Sci 55:1878–1893.
580 20. Gillooly JF. 2000. Effect of body size and temperature on generation time in zooplankton.
581 J Plankton Res 22:241–251.
582 21. Neuheimer AB, Taggart CT. 2007. The growing degree-day and fish size-at-age: The
583 overlooked metric. Can J Fish Aquat Sci 64:375–385.
584 22. Ralston DK, Keafer BA, Brosnahan ML, Anderson DM. 2014. Temperature dependence
585 of an estuarine harmful algal bloom: Resolving interannual variability in bloom dynamics
586 using a degree-day approach. Limnol Oceanogr 59:1112–1126.
587 23. Crespo BG, Keafer BA, Ralston DK, Lind H, Farber D, Anderson DM. 2011. Dynamics
588 of *Alexandrium fundyense* blooms and shellfish toxicity in the Nauset Marsh System of
589 Cape Cod (Massachusetts, USA). Harmful Algae 12:26–38.
590 24. Keafer BA, Buesseler KO, Anderson DM. 1992. Burial of living dinoflagellate cysts in
591 estuarine and nearshore sediments. Mar Micropaleontol 20:147–161.
592 25. Fischer AD. 2017. *Alexandrium catenella* Cyst Dynamics in a Coastal Embayment:
593 Temperature Dependence of Dormancy, Germination, and Bloom Initiation. PhD thesis.

Massachusetts Institute of Technology and the Woods Hole Oceanographic Institution.

26. Yamaguchi M, Itakura S, Imai I, Ishida Y. 1995. A rapid and precise technique for enumeration of resting cysts of *Alexandrium* spp. (Dinophyceae) in natural sediments. Phycologia 34:207–214.

27. Anderson DM, Fukuyo Y, Matsuoka K. 2003. Cyst methodologies. Man Harmful Mar Microalgae 165–189.

28. Schwinghamer P, Anderson DM, Kulis DM. 1991. Separation and concentration of living dinoflagellate resting cysts from marine sediments via density-gradient centrifugation. Limnol Oceanogr 36:588–592.

29. Anderson DM, Kulis DM, Doucette G, Gallagher J, Balech E. 1994. Biogeography of toxic dinoflagellates in the genus *Alexandrium* from the northeastern United States and Canada. Mar Biol 120:467–478.

30. Onofri A, Benincasa P, Mesgaran MB, Ritz C. 2018. Hydrothermal-time-to-event models for seed germination. Eur J Agron 101:129–139.

31. Bantis L. 2020. Fit distributions to censored data. MATLAB Cent File Exch.

32. Matrai P, Thompson B, Keller M. 2005. Circannual excystment of resting cysts of *Alexandrium* spp. from eastern Gulf of Maine populations. Deep Res Part II Top Stud Oceanogr 52:2560–2568.

33. Butman B, Aretxabaleta AL, Dickhudt PJ, Dalyander PS, Sherwood CR, Anderson DM, Keafer BA, Signell RP. 2014. Investigating the importance of sediment resuspension in *Alexandrium fundyense* cyst population dynamics in the Gulf of Maine. Deep Res Part II Top Stud Oceanogr 103:79–95.

34. Brown RF, Mayer DG. 1988. Representing Cumulative Germination.: 2. The Use of the

Weibull Function and other Empirically Derived Curves. Ann Bot 61:127–138.

35. Moore SK, Mantua NJ, Salathé EP. 2011. Past trends and future scenarios for environmental conditions favoring the accumulation of paralytic shellfish toxins in Puget Sound shellfish. Harmful Algae 10:521–529.

36. Anderson DM, Fachon E, Pickart RS, Lin P, Uva V, Fischer AD, Brosnahan M, McRaven L, Bahr F, Richlen ML, Lefebvre K, Grebmeier J, Danielson S, Lyu Y, Fukai Y. 2021. Evidence for massive and recurrent toxic blooms of *Alexandrium catenella* in the Alaskan Arctic. PNAS 118:e2107387118.

37. McQuoid MR, Godhe A, Nordberg K. 2002. Viability of phytoplankton resting stages in the sediments of a coastal Swedish fjord. Eur J Phycol 37:191–201.

38. Kaplan-Levy RN, Hadas O, Summers ML, Rücker J, Sukenik A. 2010. Akinetes: Dormant Cells of Cyanobacteria, p. 283. *In* Lubzens, E, Cerda, J, Clark, M (eds.), Dormancy and Resistance in Harsh Environments. Springer-Verlag Berlin Heidelberg.

39. Clegg JS. 1997. Embryos of *Artemia franciscana* survive four years of continuous anoxia: The case for complete metabolic rate depression. J Exp Biol 200:467–475.

40. Broman E, Brüsin M, Dopson M, Hylander S. 2015. Oxygenation of anoxic sediments triggers hatching of zooplankton eggs. Proc R Soc B Biol Sci 282.

41. Hamdi S, Chevallier T, Bernoux M. 2012. Testing the application of an agronomic concept to microbiology: A degree-day model to express cumulative CO2 emission from soils. Eur J Agron 43:18–23.

42. Banta GT, Giblin AE, Hobbie JE, Tucker J. 1995. Benthic respiration and nitrogen release in Buzzards Bay, Massachusetts. J Mar Res 53:107–135.

43. Shull DH, Kremp A, Mayer LM. 2014. Bioturbation, germination and deposition of

Alexandrium fundyense cysts in the Gulf of Maine. Deep Res Part II Top Stud Oceanogr 103:66–78.

44. Tobin ED, Grünbaum D, Patterson J, Cattolico RA. 2013. Behavioral and Physiological Changes during Benthic-Pelagic Transition in the Harmful Alga, *Heterosigma akashiwo*: Potential for Rapid Bloom Formation. PLoS One 8:1–15.

45. Ishikawa A, Hattori M, Ishii KI, Kulis DM, Anderson DM, Imai I. 2014. In situ dynamics of cyst and vegetative cell populations of the toxic dinoflagellate *Alexandrium catenella* in Ago Bay, central Japan. J Plankton Res 36:1333–1343.

Figure legends

Figure 1. Schematic of how to measure germination rates of a natural polyclonal population of *A. catenella* cysts. Aeration initiates the germination process, spurring quiescent cysts to germinate at their individual rates.

Figure 2. Observation schemes used in sediment slurry and cyst isolation-based germination rate measurements. (a) In sediment slurry experiments, replicate flasks are filled with approximately the same number of cysts at time 0. Flasks are incubated until removed for counting at a planned time a_i. The difference between the number of cysts observed at time 0 and a_i reflects the cumulative number of cysts that have germinated by time a_i. (b) Isolation experiments track germination of individuals through repeated observations by microscopy. Actual germination times are indicated by open circles but observations only constrain germination time as occurring between times b_{i-1} and b_i (rectangles).

Figure 3. (a) Seasonal bottom water temperature in relation to (b) the quiescent fraction of the *A. catenella* cyst bed in Roberts Cove within Nauset from 2012 through 2015. *A. catenella* cysts cycle between states of quiescence (when they will germinate if exposed to oxygen and favorable temperatures) and dormancy (when they will not). In situ dormancy data are republished from cyst isolation experiments conducted by Fischer et al. 2018 (8). Each month, cohorts of freshly-collected cysts were isolated and incubated under optimal conditions (oxygen, 15ºC, light) and the quiescent fraction of the cyst bed was assessed from the cumulative fraction of cysts that germinated after one week. Grey shading demarcates the time period when experiments in this study were conducted.

Figure 4. Example images of *A. catenella* cysts (a–c) with healthy appearances that were isolated at the beginning of isolation experiments and (d) a cyst that died during experimental incubation.

Figure 5. Cumulative germination of *A. catenella* cysts incubated in sediment slurries at different temperatures plotted as a function of (a) observation days and (b) *DD*. Data were fit to a lognormal CDF (black line) using maximum log-likelihood estimation.

Figure 6. Days needed for *A. catenella* cysts to germinate at laboratory incubation temperatures. Data from Nauset cyst populations are shown alongside previously-published data for cyst populations from Puget Sound (WA) and the western and eastern Gulf of Maine (GOM) (4, 16). All germination experiments were conducted with quiescent, subsurface (presumed anoxic) cyst

686 populations that were aerated through the creation of slurries. The lines depict the degree days to
687 median germination (DD_{50}) for each population. A similar plot was originally published in
688 Anderson et al., 2021, but not fully explained (36).
689
690 **Figure 7.** Cumulative germination of individually-isolated *A. catenella* cysts incubated in
691 different months and years at the in situ temperature. Different grayscale shades reflect the
692 month and different shapes reflect the year that clutches of cysts were collected. For comparison,
693 the range of cumulative germination observed in March 2014 by slurry experiments (Fig. 5b) is
694 marked in orange, and the datapoints corresponding to the isolation experiment conducted at the
695 same time is outlined in red.
696
697
698 ***Acknowledgements***
699 We thank Donald Anderson for helpful discussions in designing these experiments, for making
700 germination data from his 2005 publication available for reanalysis, and for providing laboratory
701 space. We also thank Stephanie Moore for making germination data from her 2015 publication
702 available for reanalysis, David Kulis for technical assistance during the development of this
703 work, Taylor Sehein for counting cysts in the sediment slurry experiment, and Finn Morrison for
704 assistance with sampling trips to Nauset. We gratefully acknowledge support to A.D.F. and
705 M.L.B. through the Woods Hole Center for Oceans and Human Health (National Science
706 Foundation grants OCE-0430724, OCE-0911031, OCE-1314642, and OCE-1840381 and
707 National Institutes of Health grants NIEHS-1P50-ES021923-01 and P01ES028938).
708

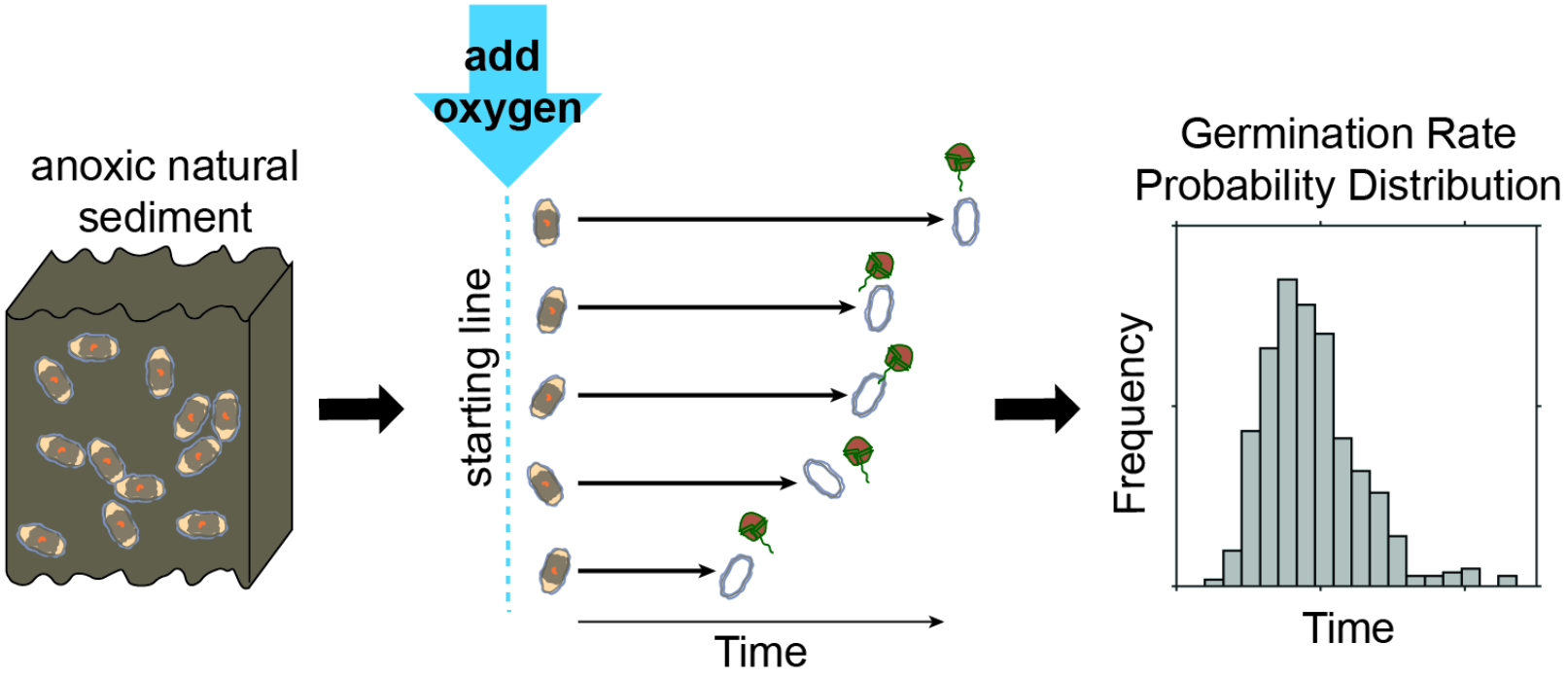
anoxic natural
sediment
add
oxygen
starting line
Time
Germination Rate
Probability Distribution
Frequency
Time

a) Sediment Slurries

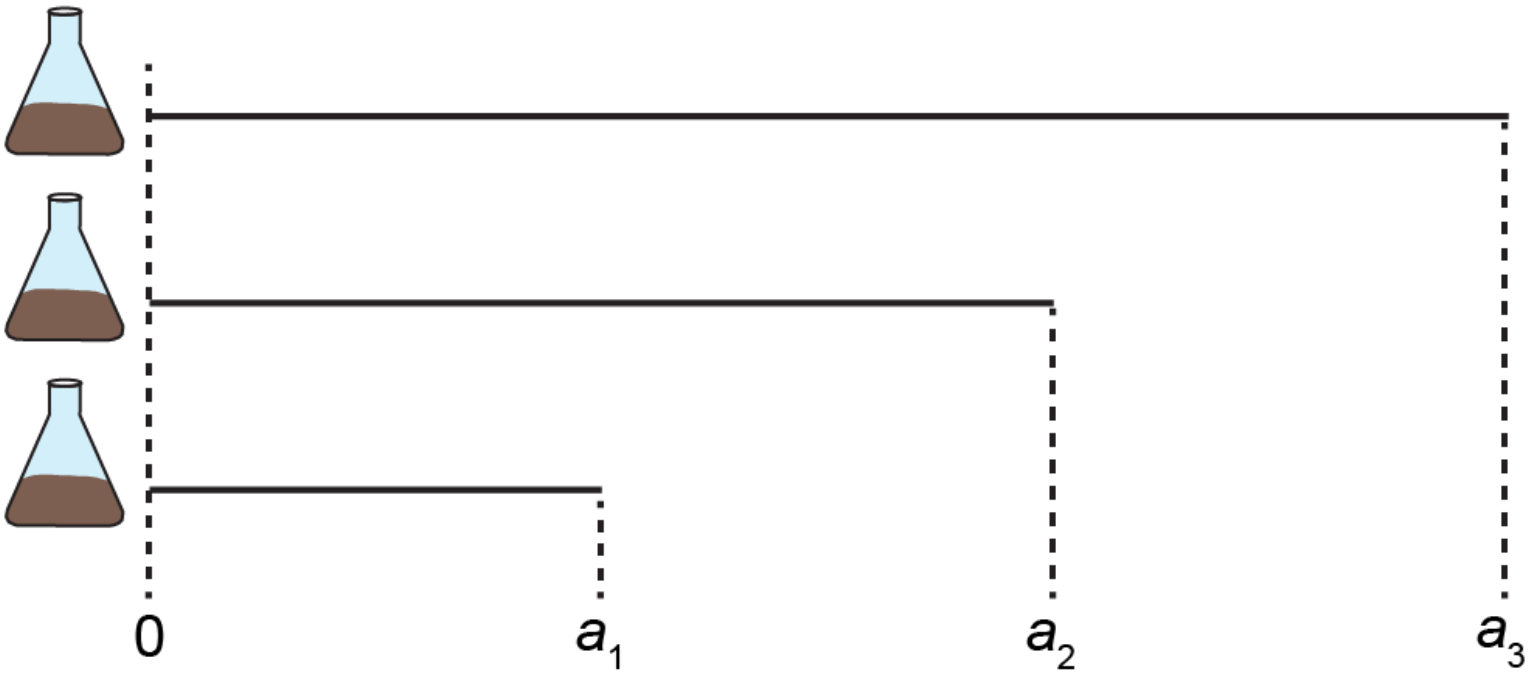

b) Cyst Isolations

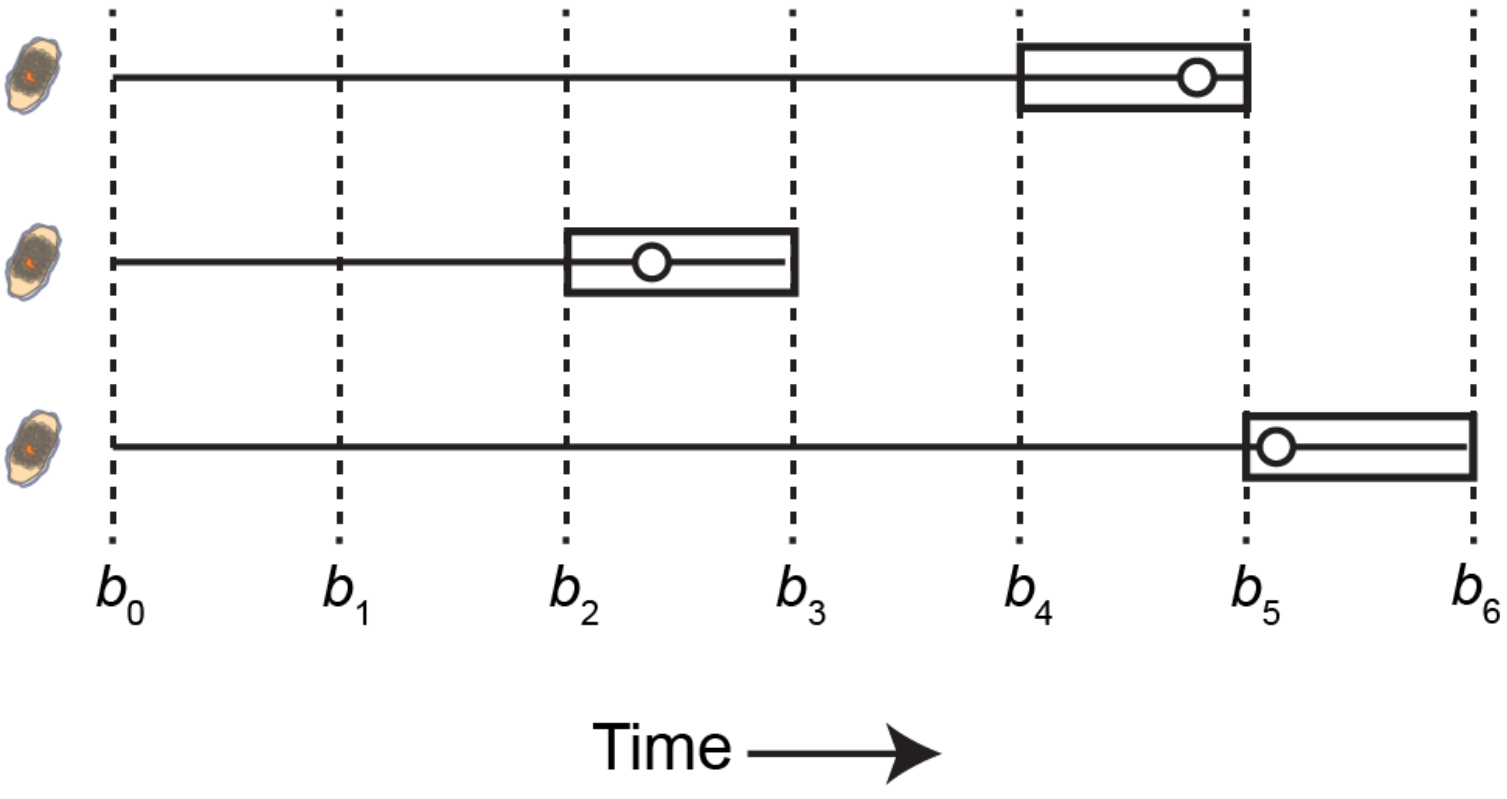

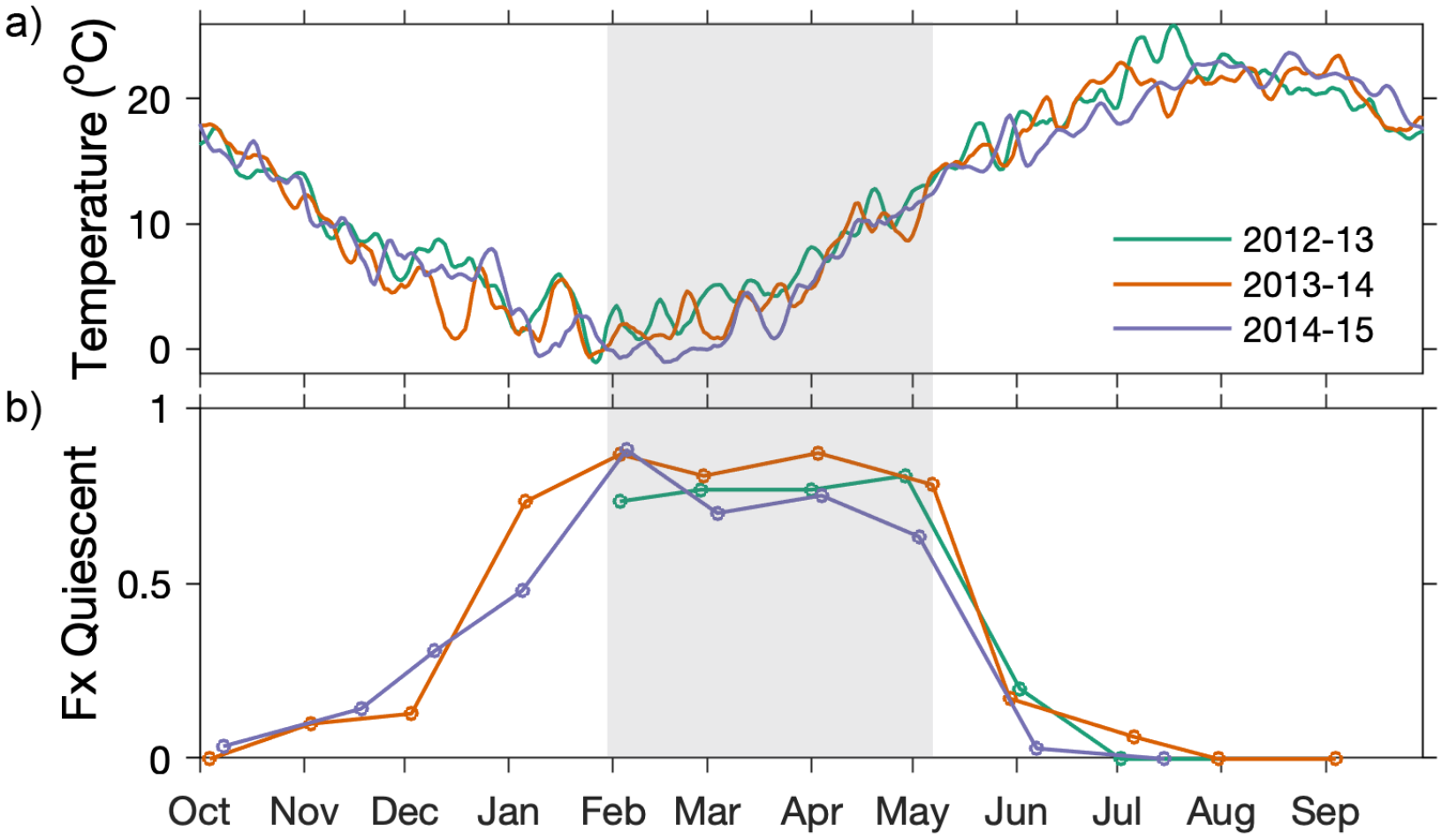
a)
Temperature (°C)
20
10
0
2012-13
2013-14
2014-15
b)
Fx Quiescent
1
0.5
0
Oct
Nov
Dec
Jan
Feb
Mar
Apr
May
Jun
Jul
Aug
Sep

a)

b)

c)

d)

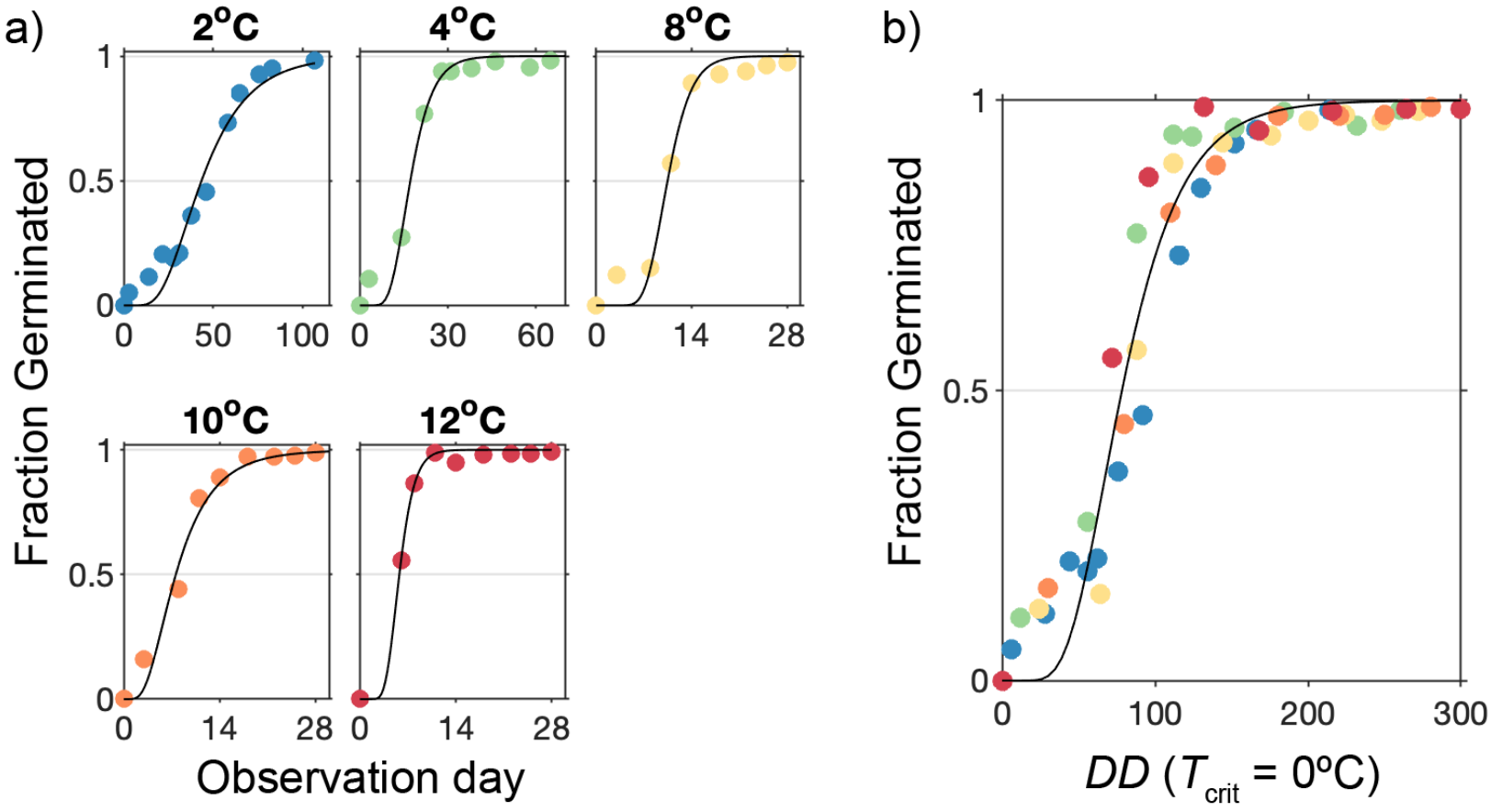
a)
2°C
4°C
8°C
10°C
12°C
Fraction Germinated
Observation day
b)
Fraction Germinated
DD (T crit = 0°C)

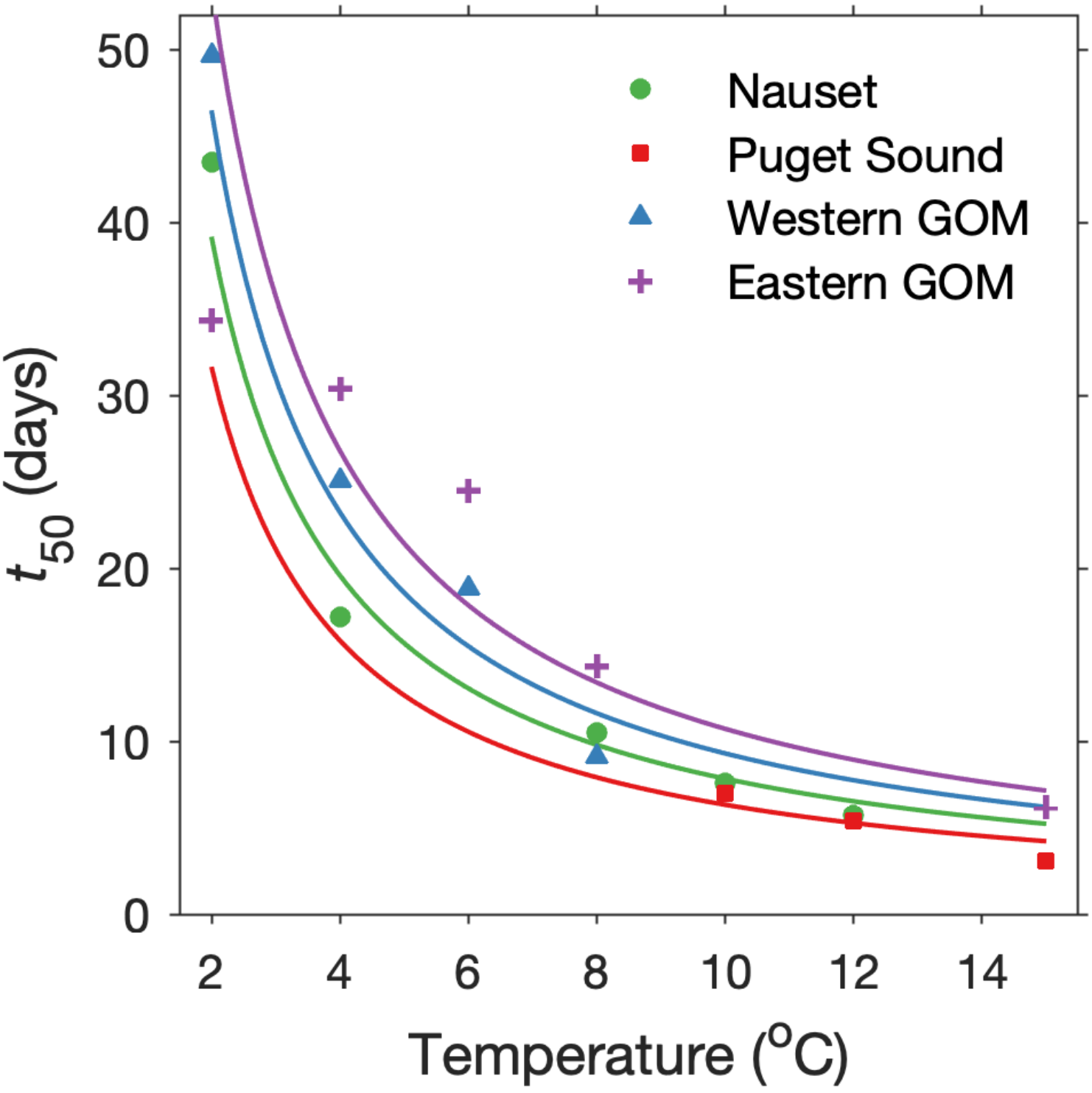
50
40
30
20
10
0
t_{50} (days)
2
4
6
8
10
12
14
Temperature (°C)
Nauset
Puget Sound
Western GOM
Eastern GOM

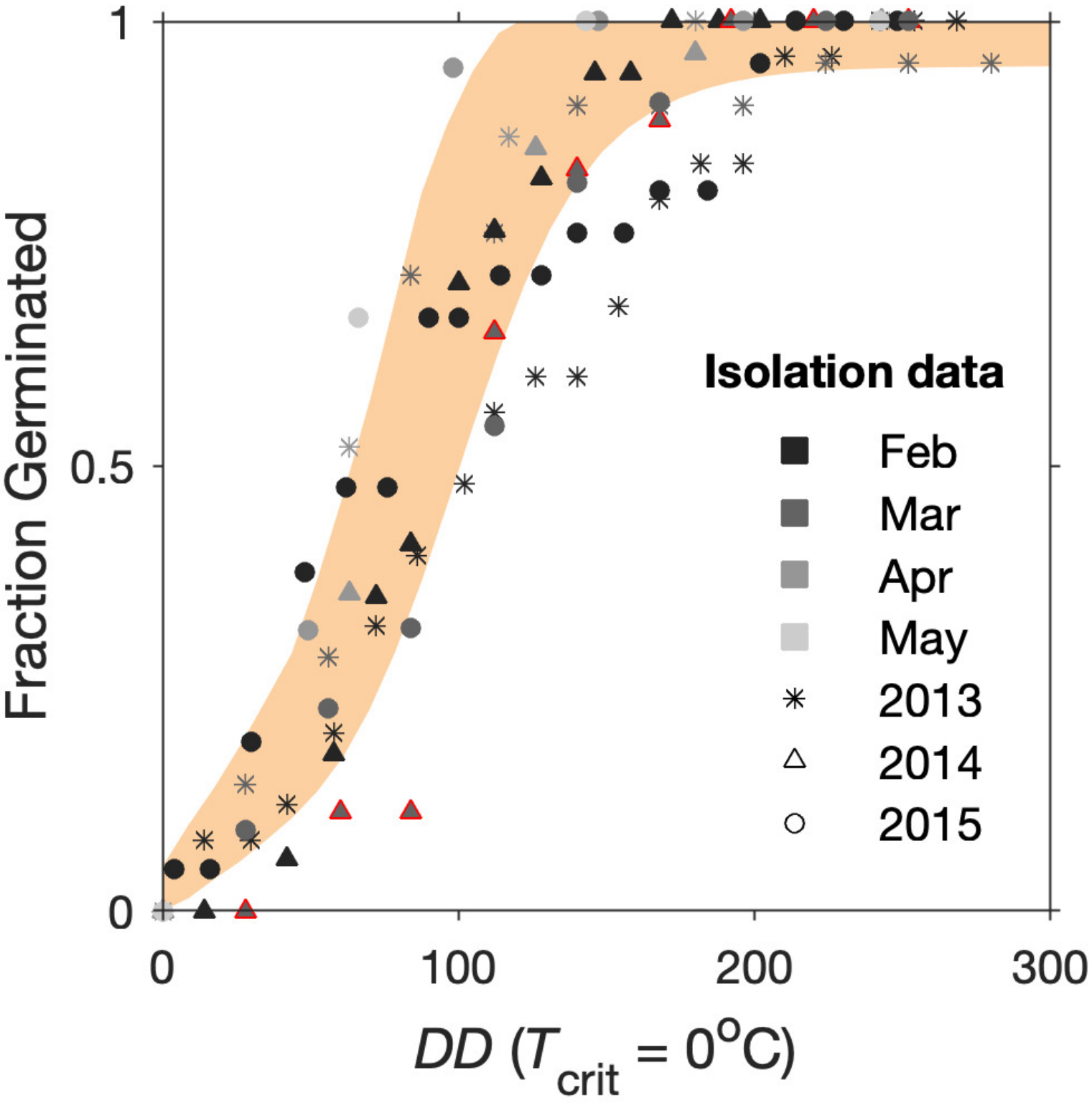
Fraction Germinated
1
0.5
0
0
100
200
300
DD (T_{crit} = 0°C)
Isolation data
Feb
Mar
Apr
May
2013
2014
2015